Published in final edited form as:
Toxicol Appl Pharmacol. 2008 August 15; 231(1): 77–84. doi:10.1016/j.taap.2008.04.014.

Effects of Mutant Human Ki-*ras*^{G12C} Gene Dosage on Murine Lung Tumorigenesis and Signaling to its Downstream Effectors

Stephanie T. Dance-Barnes[1], **Nancy D. Kock**[2], **Heather S. Floyd**[3], **Joseph E. Moore**[1], **Libyadda J. Mosley**[1], **Ralph B. D'Agostino Jr.**[4], **Mark J. Pettenati**[5], and **Mark Steven Miller**[1,6]

1*Department of Cancer Biology, Comprehensive Cancer Center, Wake Forest University School of Medicine, Winston-Salem, NC 27157.*

2*Section on Comparative Medicine, Wake Forest University School of Medicine, Winston-Salem, NC 27157.*

3*Department of Molecular Biomedical Sciences, North Carolina State College of Veterinary Medicine, Raleigh, NC 27606.*

4*Section on Biostatistics, Comprehensive Cancer Center, Wake Forest University School of Medicine, Winston-Salem, NC 27157.*

5*Department of Medical Genetics, Wake Forest University School of Medicine, Winston-Salem, NC 27157.*

Abstract

Studies in cell culture have suggested that the level of RAS expression can influence the transformation of cells and the signaling pathways stimulated by mutant RAS expression. However, the levels of RAS expression *in vivo* appear to be subject to feedback regulation, limiting the total amount of RAS protein that can be expressed. We utilized a bitransgenic mouse lung tumor model that expressed the human Ki-*ras*^{G12C} allele in a tetracycline-inducible, lung-specific manner. Treatment for 12 months with 500 μg/ml of doxycycline (DOX) allowed for maximal expression of the human Ki-*ras*^{G12C} allele in the lung, and resulted in the development of focal hyperplasia and adenomas. We determined if different levels of mutant RAS expression would influence the phenotype of the lung lesions. Treatment with 25, 100 and 500 μg/ml of DOX resulted in dose-dependent increases in transgene expression and tumor multiplicity. Microscopic analysis of the lungs of mice treated with the 25 μg/ml dose of DOX revealed infrequent foci of hyperplasia, whereas mice treated with the 100 and 500 μg/ml doses exhibited numerous hyperplastic foci and also adenomas. Immunohistochemical and RNA analysis of the downstream effector pathways demonstrated that different levels of mutant RAS transgene expression resulted in differences in the expression and/or phosphorylation of specific signaling molecules. Our results suggest that the molecular alterations driving tumorigenesis may differ at different levels of mutant Ki-*ras*^{G12C} expression, and this should be taken into consideration when inducible transgene systems are utilized to promote tumorigenesis in mouse models.

6Corresponding author: Department of Cancer Biology, 1 Medical Center Blvd., Wake Forest University School of Medicine, Comprehensive Cancer Center, Winston-Salem, NC 27157, USA Phone: 336-716-0795, Fax: 336-716-0255, E-Mail: msmiller@wfubmc.edu.

Introduction

Lung cancer is the leading cause of cancer-related deaths in both men and women in the United States. To date, less than 15% of all lung cancer patients survive >5 years (Jemal *et al.*, 2007). Non-small cell lung cancer (NSCLC), which occurs in ~75-80% of lung cancer patients, is the most common histological type of lung cancer with its subtype, adenocarcinoma (AC), being the predominant form (Jemal *et al.*, 2003). Activating mutations of Ki-*ras* occur in 30-50% of AC (Rodenhuis, 1992;Reynolds *et al.*, 1992;Mitsudomi *et al.*, 1991;Slebos *et al.*, 1991;Mills *et al.*, 1995). Thus, a better understanding of the role of Ki-*ras* in lung tumorigenesis could provide insight into the genetics, prevention, and ultimately development of novel therapies for treating this condition.

Mutations in Ki-*ras* have been shown to be an early event in both human and mouse lung tumors (Leone-Kabler *et al.*, 1997;Li *et al.*, 1994;Westra *et al.*, 1993), although clearly it is not the sole cause of cancer development. Tumorigenesis occurs following multiple genetic lesions to genes involved in cell growth, differentiation, survival, immune surveillance, metastasis, and invasion (Hanahan *et al.*, 2000), resulting from the increased expression of oncogenes and decreased expression of tumor suppressor genes. Epidemiological studies have shown NSCLC specimens contain deletions or mutations in *p53* (~50%) (Hainaut *et al.*, 1997), deletion or reduced expression of $p16^{INK4a}$ (~60%) (Serrano, 1997), and deletion or reduced expression of pRb (~30%) (Malkinson, 1998). Similar mutations are observed in murine lung tumors which exhibit deletion or reduced expression of $p16^{INK4a}$ in approximately 50% of the tumors and reduced expression of *Rb* (Tuveson *et al.*, 1999), although *p53* is rarely affected in murine lung tumors, with only a few reports occurring in late-stage tumors (Horio *et al.*, 1996;Miller, 1999).

In addition to qualitative alterations in gene structure and function resulting from mutations and deletions at key regulatory loci, quantitative changes such as amplification or overexpression of critical genes, such as *ras*, are equally important in the neoplastic process and are prevalent in a variety of human tumors (Pulciani *et al.*, 1985;Alitalo, 1984;Varmus, 1984;Mo *et al.*, 2007). Cell culture studies with NIH 3T3 cells have demonstrated that morphologic transformation of the cells occurred only when large amounts (≥10μg) of recombinant DNA molecules carrying the normal human H-*ras*-1 proto-oncogene were transfected into the cells (Pulciani *et al.*, 1985). Similar studies addressed the levels of H-ras^{wt} on transformation by comparing the phenotype of cells expressing highly elevated levels of Ha-ras^{wt} with cells expressing more modest levels of Ha-ras^{Val12} on rat cells (Ricketts *et al.*, 1988). This work showed that markedly elevated levels of Ha-ras^{wt} did not form colonies, but varied levels or doses of H-$ras^{Val\text{-}12}$ resulted in the formation of a wide-ranging number of colonies depending on the gene dosage of the mutant RAS gene. Mo *et al.* (Mo *et al.*, 2007) also demonstrated, utilizing a mouse bladder tumor model, that doubling the gene dosage of activated Ha-*ras* triggered early on-set, rapidly growing, and fully penetrant urothelial tumors throughout the urinary tract. Low level expression of constitutively active Ha-*ras* was insufficient in initiating urothelial development, even with deletion of the *Ink4a/Arf* gene locus.

Activation of Ras leads to the sequential activation of Raf, MEK, p42, and p44 MAP-ERK kinases (Finney *et al.*, 1993;Howe *et al.*, 1992). Studies in NIH 3T3 cells have shown that Raf-activated pathways are capable of eliciting distinctly different biological outcomes depending on the strength of the signal (Woods *et al.*, 1997;Sewing *et al.*, 1997). Low levels of Raf activity led to activation of cyclin D1-cdk4 and cyclin E-cdk2 complexes and to cell cycle progression, whereas higher activity levels elicited cell cycle arrest correlating with induction of $p21^{Cip1}$ and inhibition of cyclin-cdk activity. This data demonstrated the importance of evaluating not only structural but also quantitative aspects of oncogene activation when evaluating the tumorigenic potential of critical genes.

In a previous study focusing on the early events in lung AC formation, our laboratory developed and characterized a bitransgenic mouse lung tumor model that conditionally expresses the human Ki-*ras*^{G12C} allele in a doxycycline (DOX)-inducible, lung-specific manner (Floyd *et al.*, 2005). This system makes use of the inducible tet-on system (Shockett *et al.*, 1996). One strain of transgenic mice contain a reverse tetracycline (tet) *trans*-activator (rtTA) protein linked to the Clara cell secretory protein (CCSP) promoter and constitutively express the rtTA gene product specifically in the lungs (Hayashida *et al.*, 2000). The second line of transgenic mice contain the cDNA of Ki-*ras*^{G12C} cloned into the tetO$_7$-CMV plasmid, placing the mutant human Ki-*ras*^{G12C} transgene downstream of a tet-inducible promoter (Floyd *et al.*, 2005). When these two transgenic mouse strains are crossed, lung specific expression of the rtTA gene product occurs in the presence of the tet0$_7$-CMV-Ki-*ras* transgene. In the absence of DOX, the rtTA gene product was unable to recognize the tetO sequence and was thus unable to stimulate transcription. Treatment of the bitransgenic mice with DOX allowed binding of the rtTA protein to the tetO enhancer, resulting in activation of the CMV promoter and transcription of the Ki-*ras* gene specifically in the lung (Floyd *et al.*, 2005). This model appears to recapitulate the earliest stages of lung tumorigenesis, as mice treated with DOX (500 μg/ml) for 12 months develop benign foci of hyperplasia and adenomas, showing little progression to adenocarcinomas at a dose of DOX inducing maximal transgene expression (500 μg/ml in the drinking water). Examination of the lung tissue by both quantitative real-time PCR and immunohistochemistry (IHC) demonstrated alterations in the expression and/or phosphorylation of cell cycle regulatory and signal transduction genes in the tumor tissues. These alterations included elevated levels of p19^{ARF}, survivin, and cyclin D1, decreased expression of pRb, elevated RAL-GDS activity (as assessed by pull down assays), and increased phosphorylation of erk and its downstream effectors, p38 and its downstream effectors, and *p53*. Our data suggested that the Ki-*ras*^{G12C} allele activates a specific subset of downstream effector pathways and that the combination of alterations in both proliferative and anti-proliferative signaling pathways determined the benign phenotype of the lung tumors in the Ki-*ras*^{G12C} expressing mice (Floyd *et al.*, 2005;2006).

To analyze the effects of RAS gene dosage on lung tumor formation in an *in vivo* setting, we utilized the Ki-*ras*^{G12C} expressing mice and varied the levels of mutant RAS transgene expression by administering different concentrations of DOX in the drinking water. Our studies suggest that the molecular alterations driving tumorigenesis may differ at different levels of mutant RAS expression. These results, combined with earlier studies on the effects of different RAS mutations on the tumorigenic potential of the lesion, suggest that the type of mutation and the level of expression of the RAS gene determine which signaling pathways are activated or repressed during the neoplastic process and thus play a role in determining the pathological phenotype and severity of the tumor.

Materials and Methods

Animal treatment and histological analysis of lungs

The CCSP-rtTA/Ki-ras^{G12C} bitransgenic mice, as well as Ki-*ras*^{G12C} monotransgenic controls, were either untreated or treated with 25 or 100 μg/ml of DOX in the drinking water, beginning 8 weeks after birth, for 12 months. Tumor multiplicity and staging data obtained from mice treated with 25 or 100 μg/ml of DOX were compared to the multiplicity and staging data obtained previously from studies utilizing 500 μg/ml of DOX (Floyd *et al.*, 2005). The mice were euthanized by CO_2 asphyxiation and cervical dislocation. Following intratracheal cannulation, the thorax was opened and the lungs were removed *en bloc* and carefully examined for the presence of pulmonary masses with the aid of a dissecting microscope. All macroscopic pulmonary lesions were recorded. Because of the small size of the lung tumors, several tumors from the same animal were pooled and isolated from areas of the lung containing several small

tumors that consisted primarily of tumor tissue, though some normal tissue was included as well. The remainder of the lung was processed for histopathology and IHC by fixation for 24 hr in 4% chilled paraformaldehyde fixative. Following fixation, the tissue was transferred and stored in 70% ethanol until the lungs were embedded in paraffin and prepared for routine microtomy (cut at 4 microns) and hematoxylin and eosin staining. The sections were examined by an ACVP Board certified veterinary pathologist, and all proliferative lesions examined were classified with respect to standard murine pulmonary tumor characteristics (Nikitin *et al.*, 2004).

FISH Analysis

Cells derived from lung tissue of Ki-*ras*^{G12C} monotransgenic mice were grown in Amniomax culture medium (Gibco, Grand Isle NY) and harvested for metaphase spreads using standard tissue culture techniques. Cells were treated with 0.5 μg of Colcemid (Gibco) for 20 min and re-suspended in 0.075 M KCl for 8 min at 37°C, followed by 3:1 methanol:acetic acid. Slides were prepared by air-drying and were pretreated with 0.001% pepsin (Sigma, St. Louis MO) in 0.01 N HCl for 10 min., followed by fixation in 1% formaldehyde and dehydration through an ethanol series. The 1.4 kb Ki-*ras* probe was directly labeled with the Vysis Nick Translation kit (Downer's Grove, IL) in Spectrum Green according to the manufacturers' protocol. The labeled Ki-*ras* probe (200 ng) was combined with blocking probes, precipitated, and re-suspended according to the Vysis Nick Translation kit instructions. Metaphases were denatured for 2 min at 70°C in 70% formamide (Fluka, Switzerland) in 2xSSC and incubated with probe at 37°C overnight. Slides were washed according to Vysis instructions. For sequential hybridization, slides were dehydrated and co-denatured with mouse whole chromosome probes labeled with Cy3 (Pinkel *et al.*, 1986) and the slides then washed as described above. The slides were counterstained with DAPI II (Vysis) and viewed with a Zeiss Axioplan 2 fluorescent microscope. The DAPI (367 nm), Spectrum Green (FITC: 509 nm) and Cy3 (588 nm) fluors were sequentially excited by a rotating filter wheel. Metaphases were captured with software (M-Fish 3.012) which accompanied the Quips imaging system (Vysis).

Real-Time RT-PCR Analysis

Eight week old CCSP/Ki-*ras* bitransgenic mice, as well as monotransgenic Ki-*ras* mice, were either untreated or administered drinking water containing 25, 100, or 500 μg/ml of DOX for 2 weeks (transgene expression analysis) or 12 months (tumor study). To determine expression of the Ki-*ras* transgene, 30 mg of whole lung tissue was homogenized with a Polytron homogenizer in RLT lysis buffer supplied in the RNeasy Mini Kit at speed 6. For analysis of lung tumors, tumor tissue was excised as described above. Total RNA was extracted using the *RNeasy* Mini Kit (Qiagen, Valencia, CA). For RT–PCR, cDNA was initially generated from 1 μg of RNA using the iScript cDNA Synthesis Kit (Bio-Rad). One tenth of the cDNA (2 μl) was used to amplify the Ki-*ras* transgene, p19^{ARF}, survivin, and GAPDH using the iCycler (Bio-Rad) for 40 cycles with SYBR Green Supermix (Bio-Rad). To generate a standard curve, each PCR product was first cloned into the pCR2.1 TA cloning vector and verified by gene sequencing. The plasmids were then utilized to generate standard curves for each of the genes using the same primers used for the unknown samples in order to quantify the copy number of each gene by the relative standard curve method. The Ki-*ras* transgene, p19^{ARF}, survivin, and GAPDH primers are listed in Table I. Cycling conditions included an initial denaturation step at 94°C for 3 min followed by 40 cycles of den aturation at 94°C for 30 s, annealing at 66.5° C (transgene and GAPDH), 59°C (survivin), or 61°C (p19^{ARF}) for 1 min, and elongation at 72°C for 1 min. A melt curve was determined following each real-time PCR run to ensure the presence of a single product. The iCycler software determined a copy number for each of the genes for each unknown sample based on the gene-specific standard curve. The values obtained for each gene of interest were normalized to GAPDH by dividing each sample by the respective GAPDH copy number. These normalized values were averaged and the average ± standard

error. PCR efficiencies and R^2 values for the standard curves ranged from 98-103% and 0.997-0.999, respectively. Significant difference between all doses was determined by ANOVA. Significant differences between individual doses were determined by the standard *t*-test.

Immunohistochemistry

Slides were deparaffinized with 3x 5 min washes with xylene. The slides were hydrated through graded alcohols 3x 1 min each. They were then placed in distilled water for 5 min. Antigen retrieval was performed using 10 mM citrate buffer (pH 6.0) for 35 min using a steamer. The slides were cooled for 20 min and placed in distilled water for 5 min. The following primary antibodies were used: anti-cyclin D1 1:100 (Abcam Inc., Cambridge, MA); anti-$p19^{ARF}$ 1:100 (Abcam Inc. Cambridge, MA); anti-survivin 1:500 (Abcam Inc., Cambridge, MA); anti-phospho-*p53* (Ser^{389}) 1:50 (Cell Signaling Technology); anti-caspase-3 (Cell Signaling Technology, Beverly, MA); anti-phospho-SAPK/JNK (Cell Signaling Technology}, anti-phospho-p44/42 MAPK (Thr^{202}/Tyr^{204}) 1:60 (Cell Signaling Technology Beverly, MA); anti-phospho-p38 MAPK (Thr^{180}/Tyr^{182}; 12F) 1:100 (Cell Signaling Technology Beverly, MA), anti-phospho-AKT (Ser^{473}; 736E11) 1:50 (Cell Signaling Technology, Beverly, MD); and anti-Ki-67 (Abcam Inc. Cambridge, MA) Samples as well as negative controls (which lacked the primary antibody) were incubated overnight at 4°C. Slides were then washed 3x 1 min with 1x Tris buffer (Biomeda, Foster City, CA) containing 0.5% casein. A ready-to-use secondary biotinylated anti-rabbit antibody (BioGenex, San Ramon, CA) was added and the slides were incubated for 30 min at 32°C. The slides were washed 3x 1 min in Tris buffer followed by a 1:20 dilution of Streptavidin-alkaline phosphatase conjugate (BioGenex) for 30 min at 32°C. The slides were then washed 3x 1 min in Tris buffer, Vector Red substrate (Vector Laboratories, Burlingham, CA) was added for 5 min, and the slides washed 2x in 0.1 M Tris–HCl buffer (pH 8.2–8.4) and for 5 min with distilled water. The slides were counterstained with Mayer's hematoxylin for 2 min, then washed under running water for 5 min. Slides were dehydrated through graded alcohol and cleared through several changes of *p*-xylene.

Immunohistochemical Scoring and Statistical Analysis

Stained sections of lung were quantified using a digital camera attached to the image J software at 40x magnification. Magnification was scored based on the “H score” (Umemura *et al.*, 2004). Fields from each slide were randomly chosen, a grid applied, and cells that fell on the intersection of two grid lines were quantified based on their staining intensity for each selected antibody. In the modified H-score, a score of “zero” designates no stain, and a score of “three” defines the darkest stain, with scores of “one” and “two” having intermediate staining (a score of “one” being the least and “two” being the greater). For each image, 100 cells with nuclei were assessed for staining intensity and assigned a value from 0 to 3. Tissue blocks from 6 to 8 individual mice were assessed at each of the different doses of DOX (each level of transgene expression). The slides were assessed by one individual (STD-B) who was blinded to the identity of the slides to assure consistency in assigning scores.

A *mixed model approach* was performed to determine the statistical significance of the difference between normal and proliferative tissue, as well as any statistical significance between proliferative tissue derived from mice treated with the 25, 100, or 500 μg/ml dose of DOX. Scored proliferative lesions were either hyperplastic lesions or adenomas. For each tissue block, two fields of proliferative lung tissue or surrounding normal tissue were quantified and averaged. A mean count ± SE was calculated which represented the average of the scores for the proliferative tissue minus the average of the scores from the surrounding normal tissue obtained from each of the quantified sections. In this calculation, 0 would represent no difference between proliferative and normal tissue, values greater than 0 would indicate an increase in staining intensity in proliferative lesions compared to normal tissue, and negative

values would indicate a decrease in staining intensity in proliferative lesions compared to normal tissue. The higher the absolute number, the greater the difference between the proliferative and surrounding normal tissue Preliminary experiments found no differences in staining intensity of normal surrounding tissue compared to tissue isolated from control mice that had not received DOX.

Results

Effects of mutant RAS gene dosage on tumor phenotype

Previous studies from our laboratory, which described the benign tumor phenotype and altered signaling pathways resulting from maximal induction of mutant RAS gene expression, demonstrated that 22 copies of the transgene had integrated into the mouse genome (Floyd *et al.*, 2005). Thus, we sought to further characterize the site of transgene integration. Chromosomes from the Ki-*ras*^{G12C} bitransgenic mice were screened using fluorescent *in situ* hybridization to determine the integration site of the of the Ki-*ras*^{G12C} transgene. The results shown in Figure 1 demonstrated that the transgene integrated into chromosome 6, the same chromosome on which the endogenous Ki-*ras* gene is found. Interestingly, our previous studies also demonstrated that the transgene was expressed in the testes and prostate of monotransgenic mice that contained only the mutant Ki-*ras* allele and lacked the tet *trans*activator protein, although there were no morphological changes observed in either organ. The human homologs of two testes-expressed loci found on human chromosome 17 (Bibbins *et al*., 1989), as well as an additional gene that plays a role in spermatogenesis (Bryan, 1977), have been shown to map to opposite arms of mouse chromosome 6, which may explain these earlier observations (Floyd *et al.*, 2005).

The tet-inducible system allows for the regulation of transgene expression by exposing the mice to varying concentrations of DOX. Quantification by real-time RTPCR of RNAs isolated from lung tissue of bitransgenic mice treated for 2 weeks with 25, 100, or 500 μg/ml of DOX demonstrated a dose dependent increase in transgene expression, with average copy numbers of 1.42×10^{-5}, 2.43×10^{-4}, and 4.95×10^{-3}, respectively (Figure 2A). This dose dependent increase in transgene expression resulted in a dose dependent increase in tumor multiplicity (Figure 2B). Bitransgenic mice that expressed lower levels of mutant RAS exhibited tumor multiplicities of 1.7±0.4 and 2.7±0.7 compared to the historical value of 34±0.5 observed in mice that expressed maximally obtainable levels of mutant RAS expression (Floyd *et al.*, 2005), and these differences were statistically significant between the 3 groups of mice (Figure 2; $p<0.001$). Monotransgenic control mice that were treated with 25 or 100 μg/ml of DOX exhibited tumor multiplicities ≤0.5 tumors/mouse, consistent with results obtained previously with 500 μg/ml of DOX.

Our previous studies demonstrated that the total levels of Ki-*ras* expression appeared to be tightly regulated; as transgene expression increased over time, the levels of the endogenous Ki-*ras* gene decreased (Floyd *et al.*, 2005). We thus evaluated the transcript levels of endogenous Ki-*ras* and found that as transgene expression was induced to higher levels, endogenous Ki-*ras* RNA levels decreased, with copy numbers (average from two individual lung preparations) of 1.58×10^{-2}, 4.75×10^{-3}, and 3.92×10^{-4} at the 25, 100, and 500 μg/ml doses of DOX, respectively. As wild type Ki-*ras* has been shown to act as a tumor suppressor gene (Zhang *et al.*, 2001), the results suggest that reduced expression of the endogenous gene may be needed to allow the full proliferative potential of the mutant transgene to be observed (see Discussion section).

As noted above, macroscopic analysis of the lungs demonstrated significantly fewer lesions with lower levels of mutant RAS expression (Figure 2B). While the average lesion size at all three doses was <1 mm, 22% and 26% of the lesions that exhibited higher levels of transgene

expression (treatment with 100 or 500 μg/ml of DOX, respectively) were larger, ranging from 1-4 mm in size. While none of the tumors reached the carcinoma stage, there were dose dependent differences noted in the frequency of tumor types between the different levels of transgene expression. Mice exhibiting the lowest levels of mutant RAS expression (treated with 25 μg/ml of DOX) had very few microscopic lesions within the lung, and these were very small hyperplasic foci. At the two higher levels of mutant transgene expression, larger hyperplastic foci (often close to being classified as adenoma) and adenomas were observed. Figure 2C shows representative sections of the hyperplastic lesions and adenomas.

Effects of mutant RAS gene dosage on downstream signaling pathways

Because of the small size of the tumors, we were unable to obtain sufficient amounts of tumor tissue for Western blot analysis. However, immunohistochemical (IHC) analyses of lung tissue from CCSP/Ki-*ras* mice expressing different levels of mutant RAS transgene demonstrated variations between treatment groups in the expression of oncogenes and tumor suppressor genes, as well as activation of signaling pathways involved in lung tumorigenesis (Figure 3A and 3B). There was a significant increase in staining intensity for phospo-*p53* and caspase-3 in lung proliferative lesions derived from mice that expressed lower levels of mutant RAS transgene (treated with either the 25 or 100 μg/ml dose of DOX). This increased staining intensity was represented by mean counts of 23.3±18 ($p=0.03$) and 38.3±7.3 ($p=0.001$) for phospho-p53, and mean counts of 51.4±2.1 ($p<0.0001$) and 45.7±7.2 ($p<0.0001$) for caspase-3, respectively. Mice expressing the highest level of the mutant RAS transgene exhibited no statistically significant changes in either *p53* phosphorylation or the levels of cleaved caspase-3. Previous IHC results reported by our laboratory (Floyd *et al.*, 2006) indicated increased expression of phospho-*p53* in lung lesions of mice when treated with 500 μg/ml of DOX; however, this determination was made using a subjective and qualitative analysis of the IHC staining than the mixed model approach used in this study.

IHC analyses comparing surrounding normal lung tissue to proliferative tissue also revealed an increase in survivin expression in lung lesions of mice that expressed higher levels of the mutant RAS transgene (treated with 100 and 500 μg/ml of DOX), represented by mean counts of 54.7±2.3 and 16.3±1.7 , respectively. There was also an increase seen in p19 expression levels in lung lesions, but only at the highest levels of transgene expression ($p<0.001$).

Additional phospho-specific antibodies were used to examine activation of the AKT and JNK pathways. A significant increase in AKT phosphorylation was only seen in lung lesions of mice that received the 100 μg/ml dose of DOX ($p<0.001$), as compared to surrounding normal tissue. A significant increase in JNK expression ($p<0.0001$) was seen in lung lesions of mice that received the 25 μg/ml dose of DOX, represented by a mean count of 13.7±2.7. However, there was a significant decrease in JNK expression seen in lung lesions of mice that expressed higher levels of the mutant RAS transgene, represented by mean counts of −7.3±2 .5 ($p=0.004$) and −11.0±1.6 ($p<.0001$) in mice treated with 100 μg/ml and 500 μg/ml of DOX, respectively. IHC analysis was also used to examine expression levels or phosphorylation of additional proteins (Ki-67, ERK, cyclin D1, and p38). In all mice expressing the mutant RAS transgene, there was a significant increase in staining for Ki-67, phospho-ERK, cyclin D1, and phospho-p38 (Fig. 3A). Whereas the levels of phospho-ERK and cyclin D1 were maximally induced at the lowest level of transgene expression, phosphorylation of p38 and expression of Ki-67 exhibited a dose-dependent response. For phospho-p38, the staining intensity at the 25 μg/ml dose was significantly lower ($p <0.02$) than the 100 or 500 μg/ml dose; for Ki-67, the 500 μg/ml dose was significantly higher ($p < 0.0001$) than the two lower doses.

To further confirm the results obtained by IHC, we isolated mRNA from lung tumors of CCSP/Ki-ras mice treated with each of the 3 doses of DOX and normal tissue from untreated mice. Real time RT-PCR (Figure 3C) showed that the mRNA expression levels for $p19^{ARF}$ and

survivin were comparable to that of the protein levels determined by IHC analysis. Because of potential contamination from non-tumorous lung tissue, the levels of RNA expression may underestimate the actual changes in RNA levels in the tumors.

Discussion

Previous studies from our laboratory described the development and characterization of a bitransgenic mouse model that allows for the conditional expression of the mutant human Ki-*ras*^{G12C} allele in a lung-specific manner from a tetracycline regulated promoter (Floyd *et al.*, 2005). In this study, treatment of bitransgenic mice with 3 different doses of DOX resulted in a statistically significant, dose dependent increase in transgene expression (Figure 2A), as well as a dose dependent increase in tumor multiplicity (Figure 2B).

The increase in tumor multiplicity observed between the 25 and 100 μg/ml doses (1.6 fold) was much smaller than the large increase in transgene expression (17 fold). As our previous studies demonstrated that the total levels of Ki-*ras* expression are tightly regulated (Floyd *et al.*, 2005), we evaluated the levels of endogenous Ki-*ras* expression by RT-PCR. We found that as transgene expression was induced to higher levels, endogenous Ki-*ras* RNA levels decreased. While it is possible that the observed benign tumor phenotype may be due to the increased expression of the mutant transgene, wild type Ki-*ras* has been shown to exhibit tumor suppressor activity (Zhang *et al.*, 2001). Thus, it is also possible that lower levels of endogenous wild type gene expression are required before the full proliferative potential of the mutant transgene is manifested. These data cannot distinguish between these possible mechanisms and would require the use of knockout mice or siRNA silencing to definitively determine the role of the endogenous and mutant transgene expression in altering signal transduction pathways. It does appear that increased transgene expression at the two higher doses of DOX (100 and 500 μg/ml) was associated with the transition to adenoma development, as we observed predominantly small foci of hyperplasia at the lowest levels of Ki-*ras*^{G12C} expression but increased development of adenoma formation at higher levels of mutant RAS transgene expression. Since the levels of phospho-ERK and cyclin D1 were maximally induced at the lowest levels of transgene expression, but other signaling pathways exhibited dose-dependent effects, the results confirm the importance of defects in multiple signaling pathways in driving tumor progression.

p53, a classic tumor suppressor, becomes activated in response to a myriad of cellular stressors, one of which is deregulated oncogene expression (Agarwal *et al.*, 2001;Horn *et al.*, 2007). IHC demonstrated activation of the *p53* pathway at lower levels of RAS transgene expression, whereas maximal induction of mutant RAS expression demonstrated a smaller and more subtle increase in phospho-p53 (Figure 3A). It thus appears that at lower levels of mutant RAS expression, the tumor suppressor activity of *p53* is engaged and limits tumor development. Concurrently, the lower levels of transgene expression were also associated with increased caspase-3 activity; both of these signaling molecules play critical roles in stimulating apoptosis (Howe *et al.*, 1992). In contrast, there was no significant increase in phospho-*p53* and caspase-3 staining noted in the mice treated with 500 μg/ml of DOX relative to normal lung. Interestingly, IHC and real-time RT-PCR (Figure 3) also demonstrated that there was no significant change in p19^{ARF} expression at lower levels of RAS transgene expression despite the increased phosphorylation of *p53*, whereas maximal induction of mutant RAS transgene expression resulted in significant elevation of p19^{ARF} RNA and protein but no significant activation of the *p53* pathway. Thus, lower levels of mutant RAS expression appear to induce apoptosis in the lung lesions via a *p53*-dependent mechanism but do not appear to trigger up-regulation of p19^{ARF}. However, at higher levels of mutant RAS expression, activation of *p53* and induction of apoptosis were inhibited despite increased expression of p19. Along the same lines, survivin RNA expression was increased at the two higher levels of transgene expression, which likely

enhanced cell survival. Thus, the combination of increased survival signals and decreased apoptotic signals likely accounts for the enhanced tumor multiplicity and increased occurrence of adenomas observed at high levels of transgene expression.

In addition to the differential effects of RAS dosage on the survivin and *p53* pathways, dose dependent alterations in the levels of phosphorylation or expression of other RAS downstream effector pathways were also noted. We observed increased activation of the AKT pathway, as indicated by increased staining for phospho-AKT, in the lungs of mice treated with 100 μg/ml of DOX. Activation of AKT was not observed in mice treated with 25 or 500 μg/ml of DOX (Figure 3). AKT has been found to contribute to cancer progression by stimulating cell proliferation, promoting angiogenesis, inhibiting apoptosis and enhancing cell survival (Massion *et al.*, 2004;Datta *et al.*, 1997), and may contribute to the mechanism by which moderate levels of transgene expression circumvent the tumor suppressor effects of *p53* and progress to adenoma.

The c-Jun N-terminal kinase (JNK) is a member of the stress-activated protein kinase (SAPK) family that rapidly transmit mitogenic, apoptotic and other stress-related signals in mammalian cells (31,32). Different levels of mutant RAS gene dosage resulted in differential effects on JNK phosphorylation. Mice that were induced to express higher levels of transgene expression (mice treated with 100 or 500 μg/ml of DOX) exhibited a significant decrease in JNK phosphorylation in their lung lesions compared with the increased phosphorylation of JNK observed in mice that expressed lower levels of mutant RAS transgene. Sustained JNK activation is suggested to contribute to apoptotic cell death (Guo *et al.*, 1998;Pu *et al.*, 2002), and the lack of sustained JNK activation may contribute to the lack of apoptotic activity in mice that exhibited higher levels of transgene expression.

These results provide *in vivo* evidence for the differential effects of mutant Ki-*ras* expression on various parameters of lung tumorigenesis - including alterations in tumor multiplicity and signaling events – that are dependent on the levels of mutant RAS expression. The combination of proliferative and anti-proliferative signals stimulated by different levels of RAS transgene expression differentially influence the activation of downstream effector pathways that are initiated at the level of RAS activation, and thereby influence tumor characteristics. Use of this conditionally expressed RAS transgenic model will aid in our understanding of the effects of RAS expression on tumor phenotype, and will provide important information on tumor progression, clinical staging, and response to chemotherapy.

Acknowledgments

The authors would like to thank Hermina Bogerink and Beth Phifer for technical support with various histological aspects of this work, and additional thanks to Alixanna Norris for assistance with immunohistochemical quantification. Our research was supported by NCI grants CA91909 (MSM) and CA91909-S1 (STD), and funding from the American Foundation for Aging Research (GTA #31424). This work was performed in partial fulfillment for the requirements for a Ph.D. degree in the Department of Cancer Biology at the Wake Forest University Graduate School of Arts and Sciences. A preliminary report of this work was presented at the 46th annual meeting of the Society of Toxicology.

Abbreviations

AC, adenocarcinomas
AD, adenomas
CCSP, Clara cell secretory protein
DOX, doxycycline
GAPDH, glyceraldehyde-3-phosphate dehydrogenase
erk, extracellular regulated kinase
JNK, Jun kinase

MAPK, mitogen activated protein kinase
MEK, mitogen activated erk kinase
NSCLC, non-small cell lung cancer
RT-PCR, reverse transcription-polymerase chain reaction
rtTA, reverse tetracycline *trans*-activator
tet, tetracycline

Reference List

1. Agarwal ML, Ramana CV, Hamilton M, Taylor WR, DePrimo SE, Bean LJ, Agarwal A, Agarwal MK, Wolfman A, Stark GR. Regulation of p53 expression by the RAS-MAP kinase pathway. Oncogene 2001;20:2527–2536. [PubMed: 11420662]
2. Alitalo K. Amplification of cellular oncogenes in cancer cells. Med.Biol 1984;62:304–317. [PubMed: 6398390]
3. Bibbins KB, Tsai JY, Schimenti J, Sarvetnick N, Zoghbi HY, Goodfellow P, Silver LM. Human homologs of two testes-expressed loci on mouse chromosome 17 map to opposite arms of chromosome 6. Genomics 1989;5:139–143. [PubMed: 2767684]
4. Bryan JH. Spermatogenesis revisited. IV. Abnormal spermiogenesis in mice homozygous for another male-sterility-inducing mutation, hpy (hydrocephalicpolydactyl). Cell Tissue Res 1977;180:187–201. [PubMed: 872193]
5. Datta SR, Dudek H, Tao X, Masters S, Fu H, Gotoh Y, Greenberg ME. Akt phosphorylation of BAD couples survival signals to the cell-intrinsic death machinery. Cell 1997;91:231–241. [PubMed: 9346240]
6. Finney RE, Robbins SM, Bishop JM. Association of pRas and pRaf-1 in a complex correlates with activation of a signal transduction pathway. Curr.Biol 1993;3:805–812. [PubMed: 15335813]
7. Floyd HS, Farnsworth CL, Kock ND, Mizesko MC, Little JL, Dance ST, Everitt J, Tichelaar J, Whitsett JA, Miller MS. Conditional expression of the mutant Ki-rasG12C allele results in formation of benign lung adenomas: development of a novel mouse lung tumor model. Carcinogenesis 2005;26:2196–2206. [PubMed: 16051643]
8. Floyd HS, Jennings-Gee JE, Kock ND, Miller MS. Genetic and epigenetic alterations in lung tumors from bitransgenic Ki-rasG12C expressing mice. Mol.Carcinog 2006;45:506–517. [PubMed: 16482519]
9. Guo YL, Baysal K, Kang B, Yang LJ, Williamson JR. Correlation between sustained c-Jun N-terminal protein kinase activation and apoptosis induced by tumor necrosis factor-alpha in rat mesangial cells. J.Biol.Chem 1998;273:4027–4034. [PubMed: 9461593]
10. Hainaut P, Soussi T, Shomer B, Hollstein M, Greenblatt M, Hovig E, Harris CC, Montesano R. Database of p53 gene somatic mutations in human tumors and cell lines: updated compilation and future prospects. Nucleic Acids Res 1997;25:151–157. [PubMed: 9016527]
11. Hanahan D, Weinberg RA. The hallmarks of cancer. Cell 2000;100:57–70. [PubMed: 10647931]
12. Hayashida S, Harrod KS, Whitsett JA. Regulation and function of CCSP during pulmonary Pseudomonas aeruginosa infection in vivo. Am.J.Physiol Lung Cell Mol.Physiol 2000;279:L452–L459. [PubMed: 10956619]
13. Horio Y, Chen A, Rice P, Roth JA, Malkinson AM, Schrump DS. Ki-ras and p53 mutations are early and late events, respectively, in urethane-induced pulmonary carcinogenesis in A/J mice. Mol.Carcinog 1996;17:217–223. [PubMed: 8989915]
14. Horn HF, Vousden KH. Coping with stress: multiple ways to activate p53. Oncogene 2007;26:1306–1316. [PubMed: 17322916]
15. Howe LR, Leevers SJ, Gomez N, Nakielny S, Cohen P, Marshall CJ. Activation of the MAP kinase pathway by the protein kinase raf. Cell 1992;71:335–342. [PubMed: 1330321]
16. Jemal A, Cokkinides VE, Shafey O, Thun MJ. Lung cancer trends in young adults: an early indicator of progress in tobacco control (United States). Cancer Causes Control 2003;14:579–585. [PubMed: 12948289]
17. Jemal A, Siegel R, Ward E, Murray T, Xu J, Thun MJ. Cancer statistics, 2007. CA Cancer J.Clin 2007;57:43–66. [PubMed: 17237035]

18. Leone-Kabler S, Wessner LL, McEntee MF, D'Agostino RB Jr. Miller MS. Ki-ras mutations are an early event and correlate with tumor stage in transplacentally-induced murine lung tumors. Carcinogenesis 1997;18:1163–1168. [PubMed: 9214598]
19. Li ZH, Zheng J, Weiss LM, Shibata D. c-k-ras and p53 mutations occur very early in adenocarcinoma of the lung. Am.J.Pathol 1994;144:303–309. [PubMed: 8311114]
20. Malkinson AM. Molecular comparison of human and mouse pulmonary adenocarcinomas. Exp.Lung Res 1998;24:541–555. [PubMed: 9659582]
21. Massion PP, Taflan PM, Shyr Y, Rahman SM, Yildiz P, Shakthour B, Edgerton ME, Ninan M, Andersen JJ, Gonzalez AL. Early involvement of the phosphatidylinositol 3-kinase/Akt pathway in lung cancer progression. Am.J.Respir.Crit Care Med 2004;170:1088–1094. [PubMed: 15317667]
22. Miller MS. Tumor suppressor genes in rodent lung carcinogenesis-mutation of p53 does not appear to be an early lesion in lung tumor pathogenesis. Toxicol.Appl.Pharmacol 1999;156:70–77. [PubMed: 10101101]
23. Mills NE, Fishman CL, Rom WN, Dubin N, Jacobson DR. Increased prevalence of K-ras oncogene mutations in lung adenocarcinoma. Cancer Res 1995;55:1444–1447. [PubMed: 7882350]
24. Mitsudomi T, Viallet J, Mulshine JL, Linnoila RI, Minna JD, Gazdar AF. Mutations of ras genes distinguish a subset of non-small-cell lung cancer cell lines from small-cell lung cancer cell lines. Oncogene 1991;6:1353–1362. [PubMed: 1679529]
25. Mo L, Zheng X, Huang HY, Shapiro E, Lepor H, Cordon-Cardo C, Sun TT, Wu XR. Hyperactivation of Ha-ras oncogene, but not Ink4a/Arf deficiency, triggers bladder tumorigenesis. J.Clin.Invest 2007;117:314–325. [PubMed: 17256055]
26. Nikitin AY, Alcaraz A, Anver MR, Bronson RT, Cardiff RD, Dixon D, Fraire AE, Gabrielson EW, Gunning WT, Haines DC, Kaufman MH, Linnoila RI, Maronpot RR, Rabson AS, Reddick RL, Rehm S, Rozengurt N, Schuller HM, Shmidt EN, Travis WD, Ward JM, Jacks T. Classification of proliferative pulmonary lesions of the mouse: recommendations of the mouse models of human cancers consortium. Cancer Res 2004;64:2307–2316. [PubMed: 15059877]
27. Pinkel D, Straume T, Gray JW. Cytogenetic analysis using quantitative, high-sensitivity, fluorescence hybridization. Proc.Natl.Acad.Sci.U.S.A 1986;83:2934–2938. [PubMed: 3458254]
28. Pu QQ, Streuli CH. Integrin control of cell cycle: a new role for ubiquitin ligase. Bioessays 2002;24:17–21. [PubMed: 11782946]
29. Pulciani S, Santos E, Long LK, Sorrentino V, Barbacid M. ras gene Amplification and malignant transformation. Mol.Cell Biol 1985;5:2836–2841. [PubMed: 3915535]
30. Reynolds SH, Wiest JS, Devereux TR, Anderson MW, You M. Protooncogene activation in spontaneously occurring and chemically induced rodent and human lung tumors. Prog.Clin.Biol.Res 1992;376:303–320. [PubMed: 1528924]
31. Ricketts MH, Levinson AD. High-level expression of c-H-ras1 fails to fully transform rat-1 cells. Mol.Cell Biol 1988;8:1460–1468. [PubMed: 3288862]
32. Rodenhuis S. ras and human tumors. Semin.Cancer Biol 1992;3:241–247. [PubMed: 1421168]
33. Serrano M. The tumor suppressor protein p16INK4a. Exp.Cell Res 1997;237:7–13. [PubMed: 9417860]
34. Sewing A, Wiseman B, Lloyd AC, Land H. High-intensity Raf signal causes cell cycle arrest mediated by p21Cip1. Mol.Cell Biol 1997;17:5588–5597. [PubMed: 9271434]
35. Shockett PE, Schatz DG. Diverse strategies for tetracycline-regulated inducible gene expression. Proc.Natl.Acad.Sci.U.S.A 1996;93:5173–5176. [PubMed: 8643548]
36. Slebos RJ, Hruban RH, Dalesio O, Mooi WJ, Offerhaus GJ, Rodenhuis S. Relationship between K-ras oncogene activation and smoking in adenocarcinoma of the human lung. J.Natl.Cancer Inst 1991;83:1024–1027. [PubMed: 2072410]
37. Tuveson DA, Jacks T. Modeling human lung cancer in mice: similarities and shortcomings. Oncogene 1999;18:5318–5324. [PubMed: 10498884]
38. Umemura S, Itoh J, Itoh H, Serizawa A, Saito Y, Suzuki Y, Tokuda Y, Tajima T, Osamura RY. Immunohistochemical evaluation of hormone receptors in breast cancer: which scoring system is suitable for highly sensitive procedures? Appl.Immunohistochem.Mol.Morphol 2004;12:8–13. [PubMed: 15163012]

39. Varmus HE. The molecular genetics of cellular oncogenes. Annu.Rev.Genet 1984;18:553–612. [PubMed: 6397126]

40. Westra WH, Slebos RJ, Offerhaus GJ, Goodman SN, Evers SG, Kensler TW, Askin FB, Rodenhuis S, Hruban RH. K-ras oncogene activation in lung adenocarcinomas from former smokers. Evidence that K-ras mutations are an early and irreversible event in the development of adenocarcinoma of the lung. Cancer 1993;72:432–438. [PubMed: 8319174]

41. Woods D, Parry D, Cherwinski H, Bosch E, Lees E, McMahon M. Raf-induced proliferation or cell cycle arrest is determined by the level of Raf activity with arrest mediated by p21Cip1. Mol.Cell Biol 1997;17:5598–5611. [PubMed: 9271435]

42. Zhang Z, Wang Y, Vikis HG, Johnson L, Liu G, Li J, Anderson MW, Sills RC, Hong HL, Devereux TR, Jacks T, Guan KL, You M. Wildtype Kras2 can inhibit lung carcinogenesis in mice. Nat.Genet 2001;29:25–33. [PubMed: 11528387]

Figure 1.
FISH analysis and identification of the integration site of the Ki-*ras*^{G12C} transgene in metaphase spreads from cells derived from lung tissue of Ki-*ras*^{G12C} monotransgenic mice. →, denotes integration site of Ki-*ras*^{G12C} on chromosome 6.

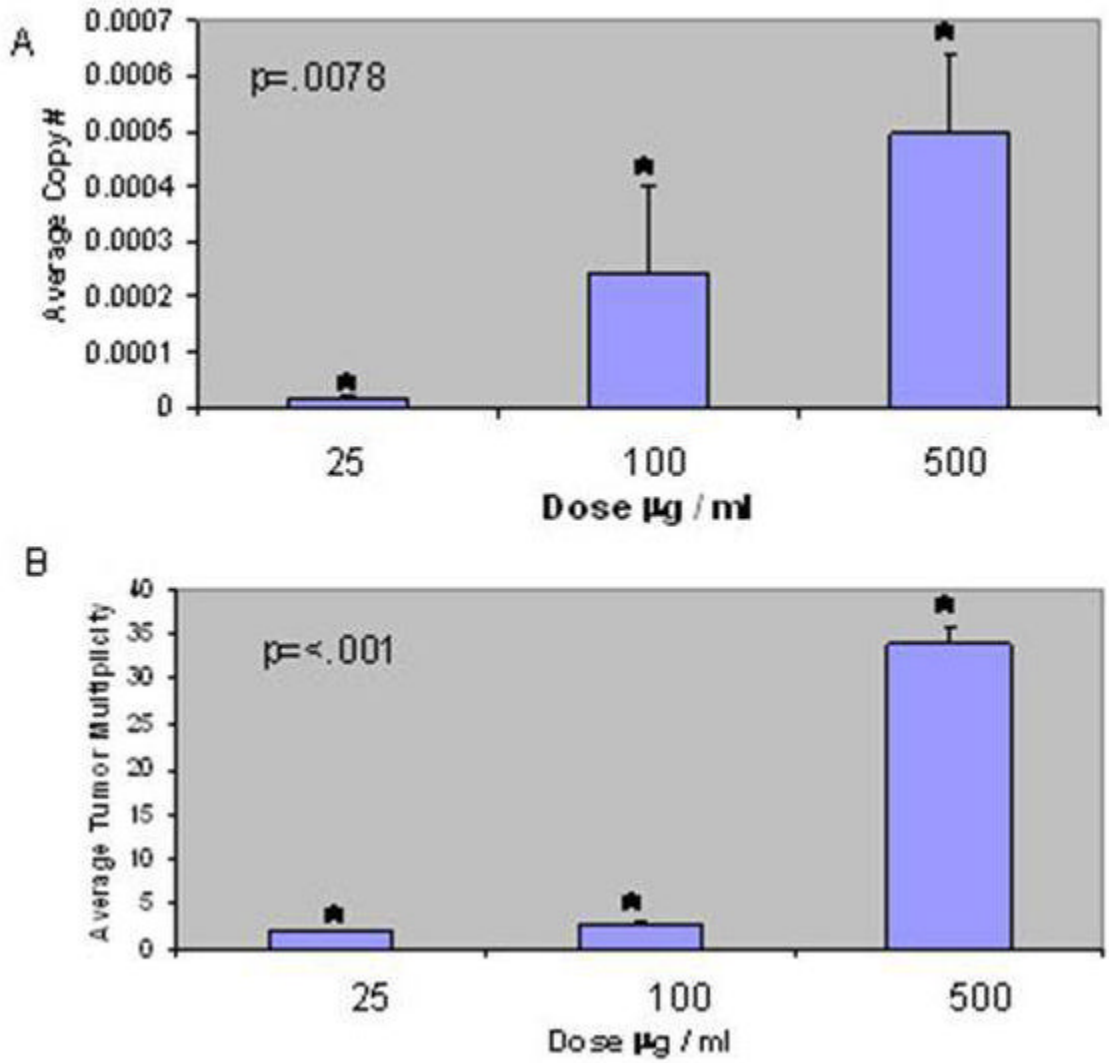

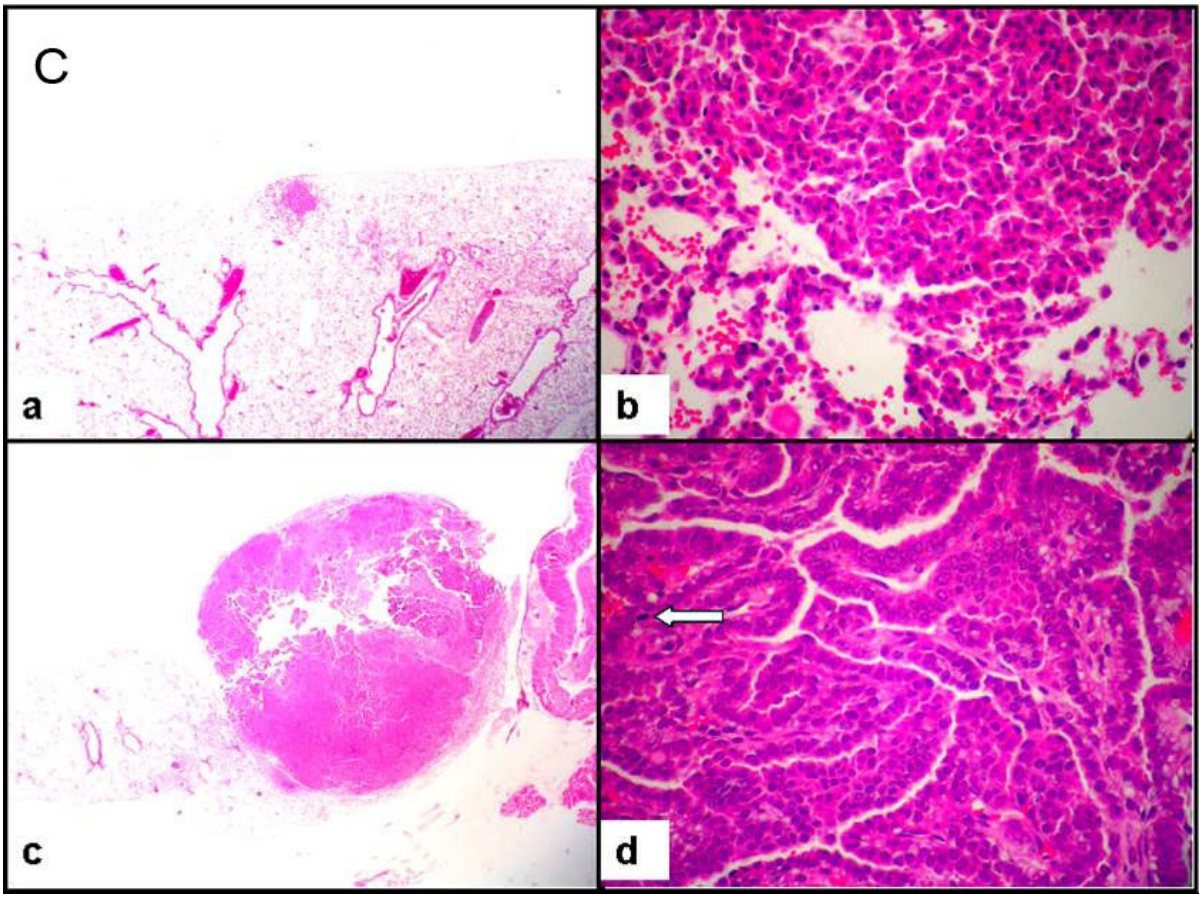

Figure 2. Transgene expression levels correlate with tumor multiplicity

(A)Total RNA was extracted from lung tissue of CCSP/Ki-*ras* mice. Real-time RT-PCR was performed to detect Ki-*ras* expression based on average copy number. Average copy number was obtained by normalizing transgene copy number to GAPDH copy number and is expressed as copy number ± SE. *, denotes s tatistical significance with p=0.0078 as determined by ANOVA and t-test. (B) Gene dosage dependent increase in tumor multiplicity, expressed as number of tumors per mouse/total number of mice with tumors ± SE. *, denotes statistical significance with $p<0.001$ as determined by ANOVA and t-test. C) Pulmonary lesions in CCSP/Ki-*ras* mice following treatment with DOX. a) Photomicrograph of a small hyperplastic focus in the lung periphery in a mouse treated with 100 μg/ml of DOX. H and E 2X; b) Higher magnification of focal epithelial hyperplasia in the lung of a mouse treated with 100 μg/ml of DOX. The cuboidal cells are uniform, without evidence of atypia, have round deeply basophilic nuclei, abundant eosinophilic cytoplasm, and maintain normal alveolar architecture. H and E 40X; c) An adenoma in the periphery of the lung of a mouse treated with 100 μg/ml of DOX. This lesion is well circumscribed, unencapsulated, quite solid, and compresses the adjacent parenchyma. H and E 2X; d) Higher magnification of an adenoma with papillary features in the lung treated with 100 μg/ml of DOX. Connective tissue fronds are covered by one to several layers of cuboidal or columnar cells which demonstrate mild anisocytosis. Nuclei are generally deeply basophilic and cytoplasm is abundant and eosinophilic. Occasionally mitosis present (arrow). H and E 40X.

A

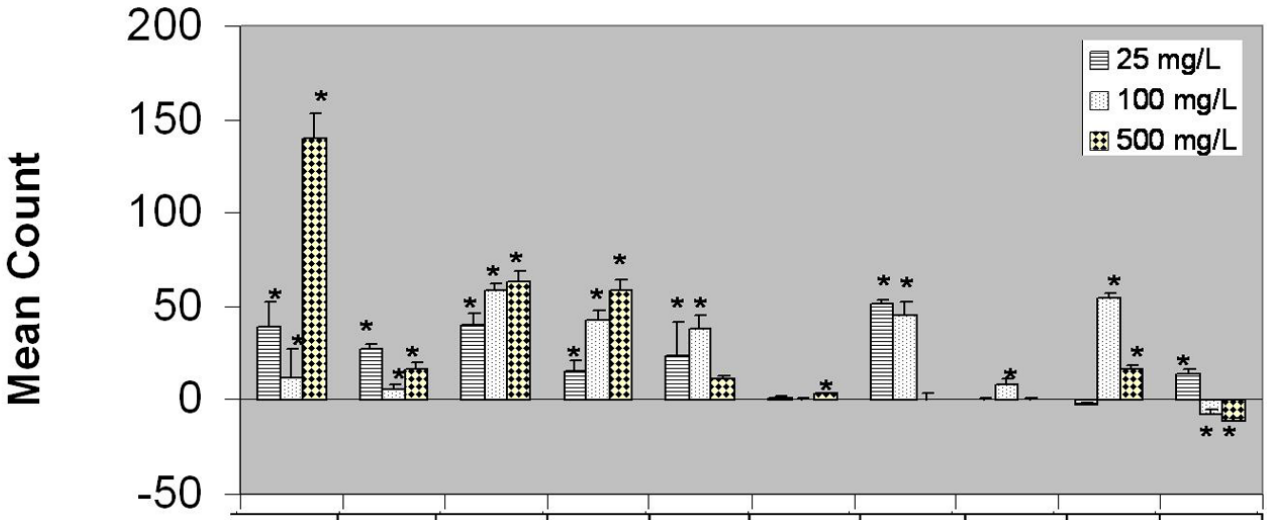

	Ki-67	p-ERK	cyclin D1	p-p38	p-p53	p19	Casp-3	p-AKT	Surv	JNK
25 mg/L	38.9 ± 13.9	27.5 ± 2.5	40.3 ± 5.5	15.5 ± 5.9	23.3 ± 18.0	1.33 ± 1.0	51.4 ± 2.1	0.00 ± 1.7	-2.17 ± 0.6	13.7 ± 2.7
100 mg/L	11.7 ± 16.0	5.7 ± 2.5	58.6 ± 4.2	42.5 ± 5.9	36.3 ± 7.3	0.50 ± 0.9	45.7 ± 7.2	8.50 ± 2.9	54.7 ± 2.3	-7.30 ± 2.5
500 mg/L	139.4 ± 13.9	16.3 ± 3.4	63.2 ± 5.5	58.5 ± 5.9	11.3 ± 1.9	3.88 ± 0.5	0.00 ± 4.2	0.00 ± 1.7	16.3 ± 1.7	-11.0 ± 1.6

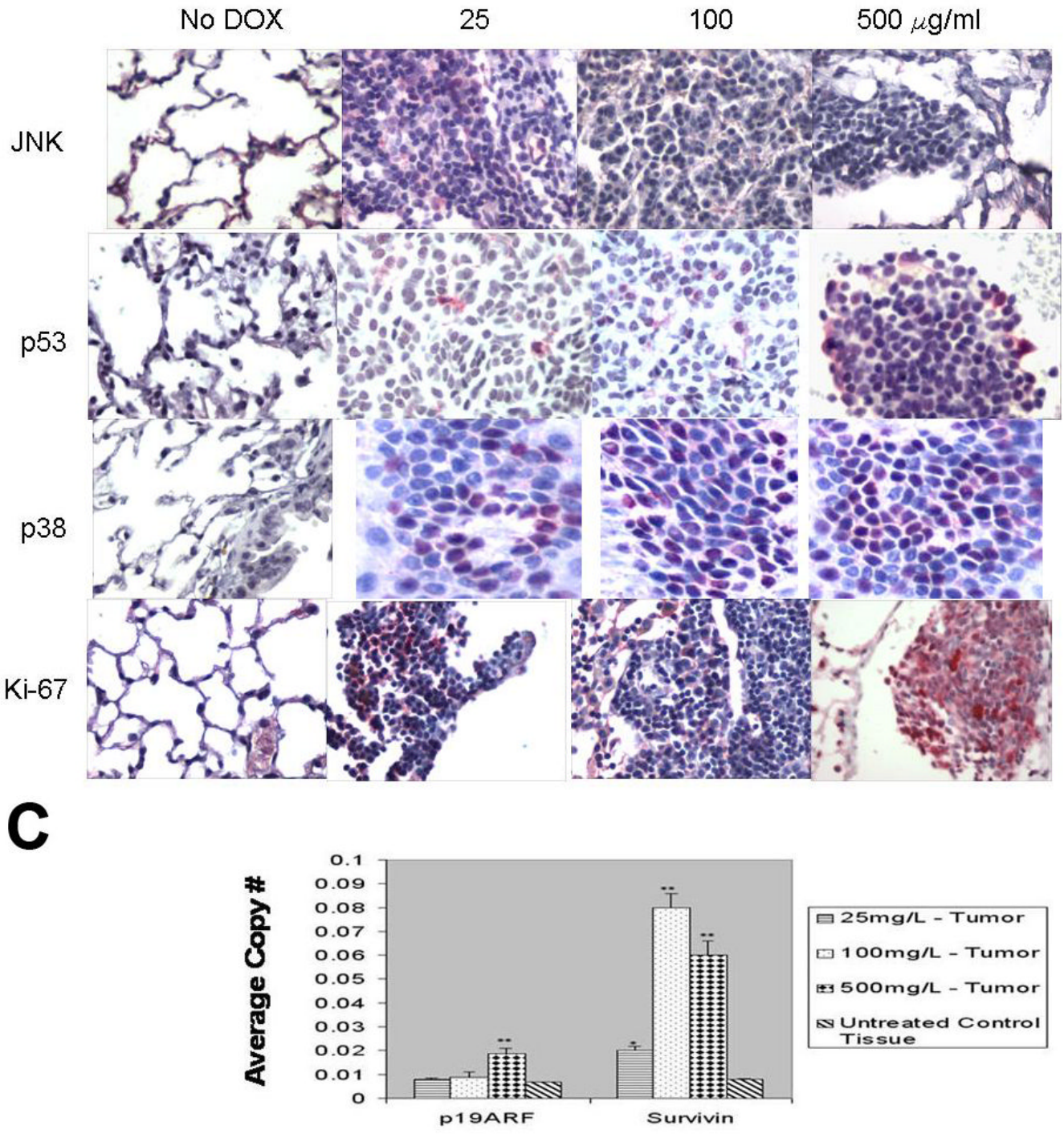

Figure 3.

A) Immunohistochemical detection and quantitation of expression or phosphorylation of RAS downstream effectors. Statistical evaluation of the immunohistochemical determination of phospho-p53, p19, caspase-3, phospho-AKT, survivin, and phospho-JNK in lung tumor tissue from bitransgenic mice treated with 25, 100, or 500 μg/ml of DOX relative to the surrounding benign tissue. A mixed model approach was utilized to determine the signal intensity; results are expressed as the mean cell counts ± the standard error. *, denotes p-values b etween the

normal and overall carcinogenic tissue was significant at ≤.05. B) Representative IHC slides showing staining with antibodies against JNK, *p53*, p38, and Ki-67 in surrounding normal tissue and lesions from mice treated with 25, 100, or 500 μg/ml of DOX; 20-40x magnification, images captured with the Image J software. C) Determination of mRNA expression of $p19^{ARF}$ and survivin. The levels of expression of $p19^{ARF}$ and survivin were determined by real-time fluorescent RT-PCR in normal lung tissue and adenomas from Ki-ras^{G12C} mice treated with 0, 25, 100, or 500 μg/ml of DOX. Each gene value is expressed as the average copy number ± SE and is corrected for the level of expression of GAPDH. Statistical differences in gene expression were determined by comparing samples from treated bitrangenic mice at each of the 3 doses to untreated bitransgenic mice (control samples). **, denotes significant difference in gene expression between treated tissue and control tissue with p value ≤ 0.05. *, denotes marginally significant difference in gene expression between treated tissue and control tissue with p value = 0.08.

Table 1

Primer sets used for real-time RT-PCR analysis

Gene	Oligonucleotide
ARF	5′ primer 5′-GGCTAGAGAGGATCTTGAGAAGAGG-3′ 3′ primer 5′-GCCCATCATCATCACCTGGTCCAGG-3′
Survivin	5′ primer 5′-GATGACAACCCGATAGAGGAGCAT-3′ 3′ primer 5′-CTCCTTTGCAATTTTGTTCTTGGCTC-3′
Ki-*ras*	5′ primer 5′ -CTGCAGAATTCGCCCTTATGACTGA-3′ 3′ primer 5′ -TAGCTGTATCGTCAAGGCACTCTTGC-3′
GAPDH	5′ primer 5′-TCTCCCTCACAATTTCCATCCCAG-3′ 3′ primer 5′-GGGTGCAGCGAACTTTATTGATGG-3′